

PRESSURE-DEPENDENCE OF TIS(2) AND TISE(2)  
 BANDSTRUCTURES(U) CORNELL UNIV ITHACA NY LAB OF ATOMIC  
 AND SOLID STATE PHYSICS G A BENESH ET AL. 22 FEB 85  
 TR-12 N00014-82-K-0576 F/G 20/12

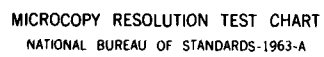
NL

UNCLASSIFIED

TR-12 N00014-82-K-0576

F/G 20/12

[illegible][illegible]



MICROCOPY RESOLUTION TEST CHART  
NATIONAL BUREAU OF STANDARDS-1963-A

AD-A151 200

OFFICE OF NAVAL RESEARCH

Research Contract No. N00014-K-0576

TECHNICAL REPORT No. 12

PRESSURE-DEPENDENCE OF  $\text{TiS}_2$  AND  $\text{TiSe}_2$  BANDSTRUCTURES

by

G. A. Benesh, A. M. Woolley and Cyrus Umrigar

Prepared for Publication

in

Physical Review Letters

Laboratory of Atomic and Solid State Physics  
Cornell University  
Ithaca, NY 14853

Reproduction in whole or part is permitted for  
any purpose of the United States Government

This document has been approved for public release  
and sale; its distribution is unlimited.

DTIC FILE COPY

DTIC  
ELECTED  
MAR 14 1985

85 03 04 075

REPORT DOCUMENTATION PAGE		READ INSTRUCTIONS BEFORE COMPLETING FORM
1. REPORT NUMBER 12	2. GOVT ACCESSION NO. AD-1151 200	3. RECIPIENT'S CATALOG NUMBER
4. TITLE (and Subtitle) Pressure-dependence of $\text{TiS}_2$ and $\text{TiSe}_2$ Bandstructures		5. TYPE OF REPORT & PERIOD COVERED Interim
		6. PERFORMING ORG. REPORT NUMBER
7. AUTHOR(s) G. A. Benesh, A. M. Woolley and Cyrus Umrigar		8. CONTRACT OR GRANT NUMBER(s) N00014-82-K-0576
9. PERFORMING ORGANIZATION NAME AND ADDRESS Laboratory of Atomic and Solid State Physics Cornell University Cornell, Ithaca, N.Y. 14853		10. PROGRAM ELEMENT, PROJECT, TASK AREA & WORK UNIT NUMBERS
11. CONTROLLING OFFICE NAME AND ADDRESS		12. REPORT DATE February 22, 1985
		13. NUMBER OF PAGES 19
14. MONITORING AGENCY NAME & ADDRESS (if different from Controlling Office)		15. SECURITY CLASS. (of this report)
		15a. DECLASSIFICATION/DOWNGRADING SCHEDULE
16. DISTRIBUTION STATEMENT (of this Report)  Approved for public release; distribution unlimited.		
17. DISTRIBUTION STATEMENT (of the abstract entered in Block 20, if different from Report)		
18. SUPPLEMENTARY NOTES  Submitted to Physical Review Letters.		
19. KEY WORDS (Continue on reverse side if necessary and identify by block number)		
20. ABSTRACT (Continue on reverse side if necessary and identify by block number) The bandstructures of the layer compounds $1\text{T-TiS}_2$ and $1\text{T-TiSe}_2$ have been calculated within the local density approximation using the self-consistent LAPW method. Both compounds are found to be semimetals with $r$ -L overlaps of 0.24 and 0.55 eV, respectively. The positioning and occupation of the bands near the Fermi level are not consistent with the carrier densities determined from Hall measurements; however agreement is obtained when the overlap is decreased by about 0.25 eV. Calculations performed with contracted lattice constants produce qualitatively the same trends in Hall coefficients as observed.		

experimentally. However, quantitative agreement can not be obtained without an overlap decrease of about 0.25 eV - indicating that  $\text{TiSe}_2$  is a semimetal and  $\text{TiS}_2$  a semiconductor.

Accession For	
NTIS GRA&I	<input checked="checked" type="checkbox"/>
DTIC TAB	<input type="checkbox"/>
Unannounced	<input type="checkbox"/>
Justification	
Distribution	
Availability	MS
For	for
at	11

AI



Pressure-dependence of  $\text{TiS}_2$  and  $\text{TiSe}_2$  Bandstructures

G. A. Benesh\*, A. M. Woolley,

Theory of Condensed Matter  
Cavendish Laboratory  
Madingley Road  
Cambridge CB3 0HE  
U. K.

and

Cyrus Umrigar

Laboratory of Atomic and Solid State Physics  
Cornell University  
Ithaca, New York 14853  
U. S. A.

Abstract

The bandstructures of the layer compounds  $1\text{T-TiS}_2$  and  $1\text{T-TiSe}_2$  have been calculated within the local density approximation using the self-consistent LAPW method. Both compounds are found to be semimetals with  $\Gamma$ -L overlaps of 0.24 and 0.55 eV, respectively. The positioning and occupation of the bands near the Fermi level are not consistent with the carrier densities determined from Hall measurements; however agreement is obtained when the overlap is decreased by about 0.25 eV. Calculations performed with contracted lattice constants reproduce qualitatively the same trends in Hall coefficients as observed experimentally. However, quantitative agreement can not be obtained without an overlap decrease of about 0.25 eV - indicating that  $\text{TiSe}_2$  is a semimetal and  $\text{TiS}_2$  a semiconductor.

\*Present address: Physics Department, Baylor University, Waco, Texas 76798  
U. S. A.

## I. Introduction

The 1T layer compounds  $\text{TiS}_2$  and  $\text{TiSe}_2$  have been intensively investigated for more than a decade, not only because of their technological uses in high energy-density batteries, but also because of their nearly or partially overlapping conduction and valence bands. The question of their intrinsic semiconducting or semimetallic bandstructures has presented a challenge to both experimental and theoretical techniques. The original optical experiments on  $\text{TiS}_2$  and  $\text{TiSe}_2$  suggested that both were semiconductors with fundamental gaps of 1-2 eV (Greenaway and Nitsche 1965); the metallic properties of each being attributed to impurities and defects. Takeuchi and Katsuta (1970a, 1970b) proposed that the metallic properties were intrinsic, resulting from the overlap of the chalcogen p and titanium d bands. For  $\text{TiS}_2$  this view has been supported by extensive resistivity experiments on highly pure samples which have revealed a  $T^2$  dependence over a range of 10-400K (Thompson 1975); by studies of the variation of the conductivity, thermopower, and lattice parameter with stoichiometry (Thompson et al 1972); and by angle-integrated photoemission experiments which have shown a long tail in the density of states indicating band overlap or a band gap of no more than 0.1 eV (Williams and Shepherd 1973, Fischer 1973). Angle-resolved photoemission (ARP) experiments have been more ambiguous in that, while they have shown overlapping bands in  $\text{TiSe}_2$  and a small gap in  $\text{TiS}_2$ , only a few bands at high-symmetry points have been resolved (Bachrach et al 1976, Traum et al 1978, Chen et al 1980, Barry et al 1983).

More recently, Hall coefficient measurements and reflectivity data, taken together, have established a strong case for a semiconducting picture for  $\text{TiS}_2$  and a semimetallic one for  $\text{TiSe}_2$  (Friend et al 1977, Logothetis et al 1979, Kukkonen et al 1981); while further resistivity measurements, showing a deviation from the previously reported  $T^2$  behaviour, have eroded much of the  $\text{TiS}_2$  semimetallic support (Kukkonen et al 1981, Klipstein et al 1983). However, within the  $\text{TiS}_2$  semiconductor model, the origin of about  $10^{20}$  electrons per  $\text{cm}^3$  in the highest purity samples, remains unknown. Wilson (1978) has suggested that excess Ti atoms might contribute more than four electrons to fill the bands, but so far this has not been supported by any evidence.

To try to clarify the experimental and theoretical pictures for these compounds, we have calculated self-consistently the bandstructures of  $\text{TiS}_2$  and  $\text{TiSe}_2$  using the Linearized Augmented Plane Wave (LAPW) method. A self-consistent (SC) approach is essential in examining these compounds since the early non-SC calculations gave gaps that were far too large: 2.0 eV  $\text{TiS}_2$ , 3.5 eV  $\text{TiSe}_2$  (Murray and Yoffe 1972); 1.4 eV  $\text{TiS}_2$ , 0.5 eV  $\text{TiSe}_2$  (Myron and Freeman 1974). More recent SC calculations have come closer to experiment: 0.23 eV gap- $\text{TiS}_2$ , 0.18 eV overlap- $\text{TiSe}_2$  (Zunger and Freeman 1977, 1978); 0.5 eV overlap- $\text{TiS}_2$  (Umrigar et al 1982); 0.80 eV overlap- $\text{TiS}_2$ , 0.95 eV overlap- $\text{TiSe}_2$  (Temmerman et al 1983). In the present work, we find semimetallic bandstructures for both  $\text{TiS}_2$  and  $\text{TiSe}_2$ , with  $\Gamma$  to L band overlaps of 0.24 and 0.55 eV, respectively.

We have also repeated the bandstructure calculations using contracted lattice constants in order to understand the differing behaviour of the  $\text{TiS}_2$  and  $\text{TiSe}_2$  Hall coefficients under pressure. We find the  $\text{TiS}_2$  Hall coefficient to be much less pressure-dependent than  $\text{TiSe}_2$ , thus qualitatively reproducing the experimental trend. However, in order to get



quantitative agreement, the evidence points to a reduction in overlap by about 0.25 eV from that calculated.

## II. Theoretical Method

The LAPW method used here has been well described in the literature (Andersen 1975, Koelling and Arbmán 1975). Briefly, the LAPW basis functions are formed by dividing real space into an interstitial region and muffin-tin (MT) spheres, then approximating the potential and solving a one-electron equation in each. The resulting solutions are joined continuously and differentiably at the region boundaries. Although a MT potential is used to construct the basis functions, so long as the basis is sufficiently complete it may be used in a variational calculation employing a potential having no shape approximations. Inside the MT spheres a semi-relativistic form of Dirac's equation is solved using a spherically averaged potential (Koelling and Harmon 1977). Both the radial solutions and their energy derivatives are included in the basis to enable the matrix elements to be independent of the energy over the range of interest. In the interstitial region the basis functions are the usual plane waves.

The total Hamiltonian  $H$  can be written as the sum,

$$H = H_{MT} + \Delta V_I + \Delta V_{NS},$$

where  $H_{MT}$  contains the kinetic, exchange-correlation, and MT potential terms,  $\Delta V_I$  is the correction potential due to non-MT terms in the interstitial region, and  $\Delta V_{NS}$  is the correction potential due to non-spherical terms inside the MT spheres.

In the present work we have included  $\Delta V_I$  exactly and  $\Delta V_{NS}$  approximately using a scheme proposed by Andersen (Jepsen et al 1982). In this approximation the plane wave expansion of the potential is continued inside the muffin-tin spheres and the spherical average subtracted from it. The new plane wave expansion differs significantly from the old only in the region just inside the MT sphere boundary. (Symmetry causes the new expansion to be small near the lattice sites.) Since the LAPW basis functions are continuous and have a continuous first derivative across the boundary, the interstitial plane waves may be used to evaluate the (approximate) non-spherical matrix elements. In testing this approximation for  $O_2$ , where the non-spherical corrections to a warped-MT potential are sizable, Umrigar found that about 90% of the eigenvalue error was eliminated. Such an approximation should be even better in a solid where the higher coordination number reduces the deviation from spherical symmetry. We have therefore utilized this approximate full-potential throughout the present work.

In iterating to self-consistency we have used a basis set consisting of approximately 150 plane waves. Exchange and correlation were treated using the Hedin-Lundqvist (1971) potential. For our Brillouin zone integrations in each iteration we have used a set of twelve special  $\underline{k}$ -points for  $D_{3d}$  symmetry derived from the six  $\underline{k}$ -point set for  $D_{6h}$  symmetry. For the densities of states, we have calculated eigenvalues over a uniform mesh of 75  $\underline{k}$ -points in the irreducible wedge of the Brillouin zone. Self-consistency was considered to be achieved when input and output potentials differed by less than 12 mRy; the eigenvalues being converged to better than 2 mRy.

### III. Results

In figures 1 and 2 are displayed our calculated bandstructures of stoichiometric  $\text{TiS}_2$  and  $\text{TiSe}_2$ , along with the corresponding densities of states. Both compounds are found to be semimetals with  $\Gamma$  to L band overlaps of 0.24 and 0.55 eV, respectively. In addition there is an indirect  $\Gamma$ -M overlap of 0.34 eV in  $\text{TiSe}_2$ , but no similar overlap in  $\text{TiS}_2$ . The Fermi energy in  $\text{TiS}_2$  falls just above a deep minimum in the DOS, in agreement with photoemission spectra (Williams and Shepherd 1973).

The strongly overlapping (0.55 eV) conduction and valence bands in  $\text{TiSe}_2$  represent the first theoretical agreement with the overlap observed in the photoemission experiments of Bachrach et al (1976). However, although the Ti d-band was not always resolved unambiguously, two other ARP studies of  $\text{TiSe}_2$  report a smaller band overlap of about 0.3 eV (Traum et al 1978, Chen et al 1980). These conflicting experimental results have not previously been reconciled. If only the latter two studies are accurate, then our calculated conduction band in  $\text{TiSe}_2$  is too low by about 0.25 eV. (We shall return to this possibility in the discussion below.) However, a reconciliation of all three ARP experiments is possible within our bandstructure: both the  $\Gamma_2^-$  and valence-band maximum  $\Gamma_3^+$  states lie near the Fermi level and are separated by 0.2 eV. The 0.3 eV overlap may then correspond to the overlap between the  $\Gamma_2^-$  and  $L_1^+$  states, while the measurement of Bachrach, et al on less-stoichiometric samples reveals the full  $\Gamma_3^+$  to  $L_1^+$  semimetallic band overlap.

The dimensions of our calculated electron pocket at L (.22 LH x .28 LA x LN) are in excellent agreement with the experimental values of .2 LH x .3 LA (Traum et al 1978) and .2 LH x .4 LA (Chen et al 1980) on higher purity  $\text{TiSe}_2$  samples. However, none of these pocket sizes are consistent with the carrier concentration of about  $2 \times 10^{20}/\text{cm}^3$  determined from Hall measurements on the best  $\text{TiSe}_2$  samples (Friend et al 1982). Our calculated

L pocket, corresponding to a concentration of  $6.6 \times 10^{20}/\text{cm}^3$ , is thus at least a factor of three too large. If the band overlap is decreased by 0.23 eV, an L pocket of size .15LH x .19LA x .70LM results, corresponding to  $2.2 \times 10^{20}$  carriers per  $\text{cm}^3$ . This is further evidence that the overlap may be overestimated by about 0.25 eV.

A similar overestimation of the band overlap may occur in our calculation for  $\text{TiS}_2$ . As previously stated, we find the bandstructure to be semimetallic with an overlap of 0.24 eV, in contradiction to the strong experimental semiconductor support. The positioning of the valence bands agrees well with recent angle-resolved photoemission experiments (see Figure 4 of Barry et al 1983). Our calculated electron pocket size of .15 LH x .19 LA x .47 LM is in fair agreement with Barry et al's highest-purity sample pocket size of .06 LH x .17 LA, since the ARP results depend upon the contour criterion chosen (this at half-maximum intensity) and the angular acceptance of the analyser ( $2^\circ$  corresponding to .06 LH). Unlike  $\text{TiSe}_2$ , the carrier concentration corresponding to this occupation ( $1.6 \times 10^{20}$ ) is very close to that determined from the Hall coefficient ( $1.4 \times 10^{20}$ ). However, if  $\text{TiS}_2$  is truly a semiconductor, then the origin of these carriers in the experimental samples must be impurities or structural defects - not the band overlap found here.

Earlier  $\text{TiS}_2$  ARP measurements found an electron pocket of size .2 LH x .4 LA (Chen et al 1980); but it was supposed that this larger electron occupation was also due to the presence of impurities and defects. If we increase the occupation of our electron pocket at L by raising the Fermi energy (corresponding to the addition of impurity or defect atoms), then we find that the Fermi level is pushed entirely out of the valence band before a pocket of size equal to the ARP data is reached. Evidence, then, of only one carrier type in the less-stoichiometric  $\text{TiS}_2$  samples is not definitive

in characterizing the bandstructure as semiconducting (Logothetis et al 1979, Kukkonen et al 1981). However, similar evidence on much purer samples does provide evidence that  $\text{TiS}_2$  is either a semiconductor or a small band overlap (less than 0.15 eV) semimetal.

In tables 1 and 2 we compare the present results with those of previous calculations. Our measured conduction and valence band widths are in good agreement with those of Zunger and Freeman (1977, 1978) using a self-consistent LCAO method. Our calculated direct and indirect gaps and overlaps are intermediate between Zunger and Freeman's and those calculated by Temmerman, et al (1983) using the self-consistent LMTO method. Both our results and those of Temmerman et al are semi-relativistic, while Zunger and Freeman's are non-relativistic.

It is interesting to note that although the majority of early calculations have tended to over-estimate the valence band (VB) - conduction band (CB) separation (some by as much as 1 eV), the most recent self-consistent calculations have tended to swing the other way. The gap now appears to be underestimated not only in  $\text{TiS}_2$  and  $\text{TiSe}_2$ , but in other complex compounds such as  $\text{ScP}$  (Wimmer et al 1979) and the rare-earth monophosphides (Hasegawa 1980). It is in no way clear that the continued disagreement with experiment as to the exact measure of band gap or overlap is due to the inferiority of present methods. Instead, the problem may be related to the well-known underestimation of semiconductor band gaps (by 40% or more) within the local density approximation (see Perdew and Levy 1983, and references therein).

In order to understand the effects of pressure upon the one-electron bandstructure, we have performed calculations using contracted lattice constants for both  $\text{TiS}_2$  and  $\text{TiSe}_2$ . Since the compressibilities of these two compounds have not been measured, we have substituted those of the layered

compounds  $\text{NbS}_2$  and  $\text{NbSe}_2$  (Jones et al 1972). When these compressibilities are extrapolated to 20 kbar (where the calculations were performed), one obtains contractions of .32% and 2.2% for the  $\text{TiS}_2$  a and c lattice spacings, and .32% and 3.2% for  $\text{TiSe}_2$ . Although we cannot expect the Nb compounds to reproduce exactly the  $\text{TiS}_2$  and  $\text{TiSe}_2$  compressibilities, we do expect the S to Se trend (less compressible S, more easily compressed Se) to be closely the same.

Our contracted bandstructures are displayed with dashed lines in figures 3 and 4. To illustrate the changes due to increasing pressure, we have shifted the energy scales so that the lowest conduction bands align at  $\Gamma$ . The most interesting feature of these bandstructures is the fact that there is almost no variation either in the p-d overlap or in the shape of the lowest conduction band in  $\text{TiS}_2$ , but that both a modified conduction band and an increased overlap (of 0.2 eV) are observed in  $\text{TiSe}_2$ .

The nature of these differences may be understood by comparing the four bands at  $\Gamma$  nearest the Fermi energy. In both uncompressed compounds the lowest lying state is the  $2^-$ , which is composed primarily of chalcogen  $p_z$  orbitals combined to form a state that is antibonding both within and between layers. Extending into the interlayer region as it does, this state is the most sensitive to any reduction in the c lattice spacing. In both  $\text{TiS}_2$  and  $\text{TiSe}_2$  the main effect of the 20 kbar of pressure is the shift of this band relative to the other three. In  $\text{TiS}_2$ , the shift is just up to the  $3^-$  state at the top of the valence band. However in  $\text{TiSe}_2$  the  $2^-$  shifts through the valence-band maximum  $3^+$  state to become the top valence band in the compressed structure. (The ordering of these bands was confirmed by setting the LAPW energy parameters equal to the Fermi energy. Thus, inside the MT's the semi-relativistic equations were solved at precisely the energy of interest, as in the APW method.) It is primarily this shift of the  $2^-$  above the  $3^+$  state

that causes the increase in the  $\text{TiSe}_2$  band overlap. This difference in  $2^-$  positioning in the two compounds is maintained even when the bands overlap less strongly than our calculations here indicate. (We determined this by repeating the calculations using an unphysical Xu exchange potential with  $\alpha=1$ .)

Interpreted in terms of the Hall coefficient, these results show that with the Fermi energy near the top of the valence band in (impure)  $\text{TiS}_2$ , the pressure-induced valence-band shifts have little effect on the measured Hall coefficient ( $<5\%$ ). In contrast, because the  $\text{TiSe}_2$  Fermi energy lies within the valence band even with similar numbers of impurities or defects, pressure-induced shifts increase the electron occupation at L causing the Hall coefficient to decrease over the entire pressure range of 20 kbar. At higher pressures we expect the  $\text{TiS}_2$   $\Gamma_2^-$  state to push through the Fermi level so that the carrier concentration will begin to rise and the magnitude of the Hall coefficient to decrease in much the same way as observed in  $\text{TiSe}_2$ . However, for nearly pure  $\text{TiS}_2$  samples, the percentage change in Hall coefficient surpasses 10% - in disagreement with experiment (Friend et al 1977). Thus, even though we observe a much smaller pressure variation of the band occupancy in  $\text{TiS}_2$ , we are not able to account for the measured constancy of the Hall coefficient. Thus, the difference in the pressure-dependence of the Hall coefficient between  $\text{TiS}_2$  and  $\text{TiSe}_2$  may not entirely be attributed to differences in the band shifts of two semimetals; the evidence points to  $\text{TiS}_2$  being a semiconductor and  $\text{TiSe}_2$  being a semimetal.

In summary, we have calculated the electronic bandstructures of  $\text{TiS}_2$  and  $\text{TiSe}_2$  self-consistently within the local density approximation, finding them to be semimetals in agreement with other recent calculations (Urrigar et al 1982 and Temmerman et al 1983). The potential has been treated

accurately, and we believe that any residual shape approximation has little effect on the band overlap. The positioning and occupation of the bands near the Fermi energy are not consistent with the carrier densities determined from Hall measurements, however, good agreement is obtained when the band overlap is decreased by 0.25 eV. Pressure-induced shifts in the semimetallic bandstructure reproduce qualitatively the same trends as the Hall data; however, quantitative agreement cannot be achieved without a decrease in the calculated overlap. This analysis points to  $\text{TiS}_2$  being a semiconductor and  $\text{TiSe}_2$  being a semimetal.

Acknowledgments:

The authors gratefully acknowledge stimulating conversations with Roger Haydock through the course of this work. GAB acknowledges the tenure of a SERC - Research Assistantship and a Baylor University summer sabbatical. CU acknowledges the support of the Office of Naval Research.



References:

- Andersen O K 1975 Phys. Rev. B 12 3060
- Bachrach R Z, Skibowski M and Brown F C 1976 Phys. Rev. Lett. 37 40
- Barry J J, Hughes H P, Klipstein P C and Friend R H 1983 J. Phys. C 16 393
- Bullett D W 1978 J. Phys. C 11 4501
- Chen C H, Fabian W, Brown F C, Woo K C, Davies B, Delong B and Thompson A H  
1980 Phys. Rev. B 21 615
- Fischer D W 1973 Phys. Rev. B 8 3576
- Friend R H, Jerome D, Liang W Y, Mikkelsen J C and Yoffe A D 1977 J. Phys.  
C 10 L705
- Greenaway D L and Nitsche R 1965 J. Phys. Chem. Solids 26 1445
- Hasegawa A 1980 J. Phys. C 13 6147
- Hedin L and Lundqvist B I 1971 J. Phys. C 4 2064
- Ismaki H and von Boehm J 1981 J. Phys. C 14 L75
- Ismaki H, von Boehm J and Krusius P 1979 J. Phys. C 12 3239
- Jepsen O, Madsen J and Andersen O K 1982 Phys. Rev. B 26 2790
- Jones R E Jr, Shanks H R, Finnermore D K and Morosin B 1972 Phys. Rev. B 6  
835
- Klipstein P C and Friend R H 1983 Submitted for publication
- Koelling D D and Arbman G O 1975 J. Phys. F 5 2041
- Koelling D D and Harmon B N 1977 J. Phys. C 10 3107
- Krusius P, von Boehm J and Ismaki H 1975 J. Phys. C 8 3788
- Kukkonen C A, Kaiser W J, Logothetis E M, Elumenstock B J, Schroeder  
P A, Faile S P, Colella R and Gambold J 1981 Phys. Rev B 24 1691
- Logothetis E M, Kaiser W J, Kukkonen C A, Faile S P, Colella R and Gambold  
J 1979 J. Phys. C 12 L521
- Murray R B and Yoffe A D 1972 J. Phys. C 5 3038
- Myron H W and Freeman A J 1974 Phys. Rev. B 9 481

- Perdew J P and Levy M 1983 Phys. Rev. Lett. 51 1884
- Shepherd F R and Williams P M 1974 J. Phys. 7 4416
- Takeuchi S and Katsuta H 1970a J. Jap. Inst. Metals 34 758
- 1970b J. Jap. Inst. Metals 34 764
- Temmerman W, Glotzel D and Andersen O K 1983 unpublished
- Thompson A H 1975 Phys. Rev. Lett. 35 1786
- Thompson A H, Pisharody H R and Koehler R F 1972 Phys. Rev. Lett. 29 163
- Traum M M, Margaritondo G, Smith N V, Rowe J E and DiSalvo F J 1978 Phys. Rev. B 17 1836
- Unger C, Ellis D E, Wang D-s, Krakauer H and Posternak M 1982 Phys. Rev. B 26 4935
- Williams P M and Shepherd F R 1973 J. Phys. C 6 136
- Wimmer E, Neckel A, Schwarz K and Eibler R 1979 J. Phys. C 12 5453
- Zunger A and Freeman A J 1977 Phys. Rev. B 15 906
- Zunger A and Freeman A J 1978 Phys. Rev. B 17 1839

Table 1: Comparison of  $\text{TiS}_2$  band widths and gaps  
obtained by different self-consistent (SC) and non-SC methods

	KKR <sup>a</sup>	OPW-SC <sup>b</sup>	AO <sup>d</sup>	LCAO-SC <sup>e</sup>	LMT0-SC <sup>f</sup>	LAPW-SC <sup>g</sup>
p-width (VB2)	5.0eV	6.6eV	6.1eV	5.5eV	5.6eV	5.5eV
d-width (CB)	2.7	7.1	3.3	4.6.	5.0	4.4
lower CB width (CB1)	1.5	4.3		2.5	2.2	2.0
upper CB width (CB2)	1.0			1.1	1.7	1.5
CB2-CB1	0.2			0.3	0.9	0.7
Centre of Gravity CB1-CB2	1.2			2.3	2.4	2.3
lower VB width (VB1)		2.5	2.6	1.9	2.0	2.0
VB2-VB1		5.5	5.9	6.8	5.9	6.4
VB maximum	$\Gamma_3^-$	$\Gamma_3^-$	$\Gamma_3^-$	$\Gamma_2^-$	$\Gamma_3^-$	$\Gamma_3^-$
CB minimum	$L_1^+$	$L_1^+$	$L_1^+$	$L_1^+$	$L_1^+$	$L_1^+$
$\Gamma$ Direct Gap	2.0	3.7	1.3	0.84	0.02	0.28
M Direct Gap	2.8	3.7	2.0	2.5	1.4	1.7
L Direct Gap	2.3	3.4	1.3	1.6	0.5	1.1
$\Gamma$ -M Ind. Gap	1.5	1.6		0.29	-0.27	0.02
$\Gamma$ -L Ind. Gap	1.4	1.5 (0.64) <sup>c</sup>	0.7	0.23	-0.80	-0.24

<sup>a</sup>Myron and Freeman 1974

<sup>b</sup>Krusius et al 1975

<sup>c</sup>Isomaki and von Roehm 1981

<sup>d</sup>Bullett 1978

<sup>e</sup>Zunger and Freeman 1977

<sup>f</sup>Temmerman et al 1983

<sup>g</sup>Present work

Table 2: Comparison of  $\text{TiSe}_2$  band widths and gaps  
obtained by different self-consistent (SC) and non-SC methods

	KKR <sup>a</sup>	OPW-SC <sup>b</sup>	AO <sup>d</sup>	LCAO-SC <sup>e</sup>	LMT0-SC <sup>f</sup>	LAPW-SC <sup>g</sup>
p-width (VB2)	5.9eV	6.4eV	6.3eV	5.8eV	6.6eV	5.7eV
d-width (CB)	2.7		3.4	4.1	3.4	4.1
lower CB width (CB1)	1.5			2.3	1.9	1.9
upper CB width (CB2)	1.0			1.7	1.4	1.6
CB2-CB1	0.2			0.3	0.9	0.6
Centre of Gravity CB2-CB1				2.1	3.2	2.2
lower VB width (VB1)		2.4	2.9	2.2		1.8
VB2-VB1		5.1	6.1	6.9		6.9
VB maximum	$\Gamma_3^-$	$\Gamma_3^-$	$\Gamma_3^-$	$\Gamma_3^-$	$\Gamma_3^+$	$\Gamma_3^+$
CB minimum	$L_1^+$	$L_1^+$	$L_1^+$	$L_1^+$	$L_1^+$	$L_1^+$
$\Gamma$ Direct Gap	1.2	3.5		0.35	0.0	0.13
M Direct Gap	2.4	3.5		2.0	1.1	1.4
L Direct Gap	0.8	3.4		1.3	0.12	0.86
$\Gamma$ -M Ind. Gap	0.8	2.0		0.15	-0.47	-0.32
$\Gamma$ -L Ind. Gap	0.5	1.5 (0.32) <sup>c</sup>	0.1	-0.18	-0.95	-0.55

<sup>a</sup>Myron and Freeman 1974

<sup>b</sup>Isomaki et al 1979

<sup>c</sup>Isomaki and von Boehm 1981

<sup>d</sup>Bullett 1978

<sup>e</sup>Zunger and Freeman 1978

<sup>f</sup>Termerman et al 1983

<sup>g</sup>Present work

Figure Captions:

1.  $\text{TiS}_2$  bandstructure and total density of states.
2.  $\text{TiSe}_2$  bandstructure and total density of states.
3.  $\text{TiS}_2$  bandstructure near the Fermi energy calculated with uncompressed (solid line) and compressed (dashed line) lattice constants. Energy divisions are in electron volts.
4.  $\text{TiSe}_2$  bandstructure near the Fermi energy calculated with uncompressed (solid line) and compressed (dashed line) lattice constants. Energy divisions are in electron volts.

Figure 1

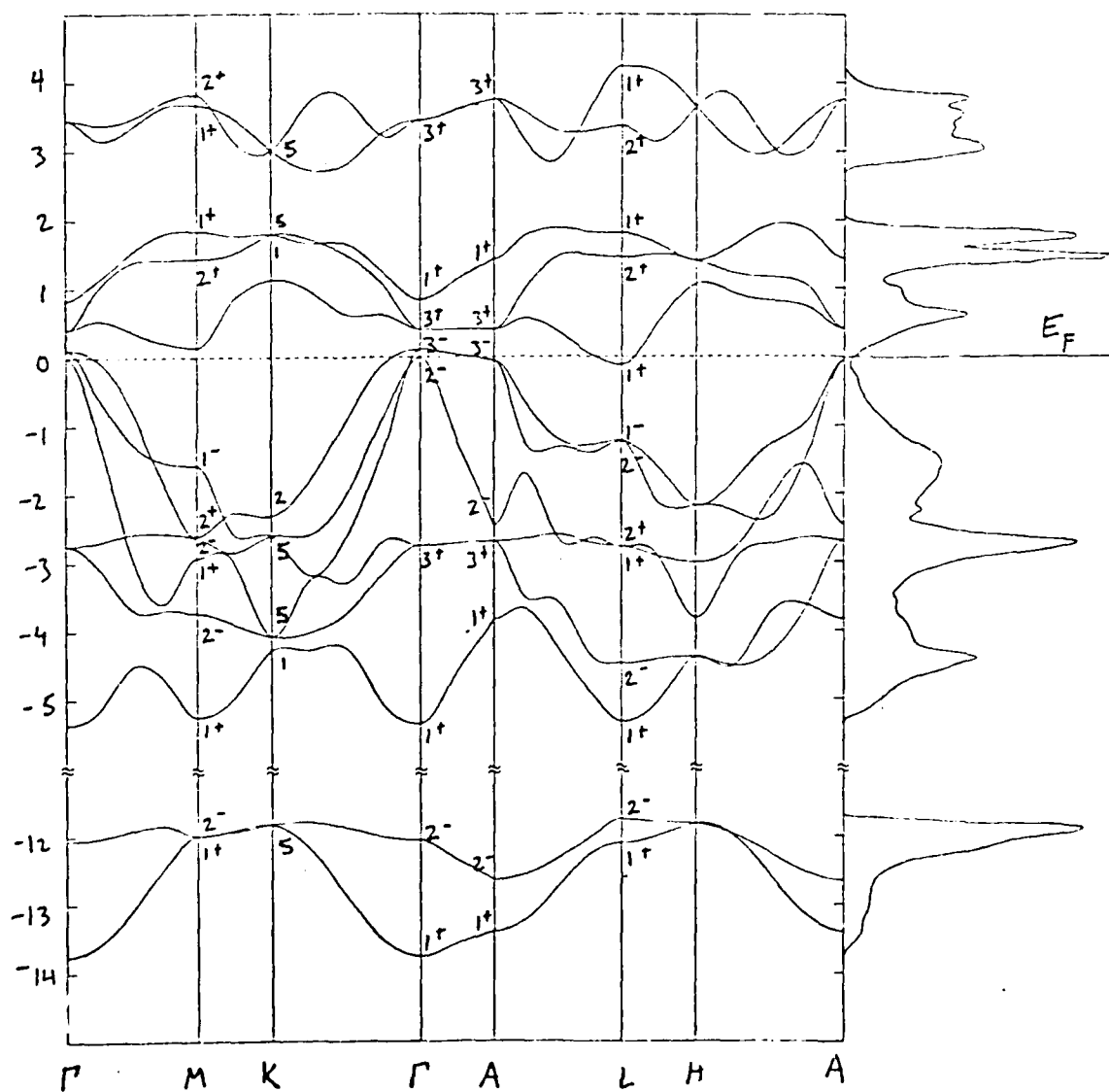


Figure 2

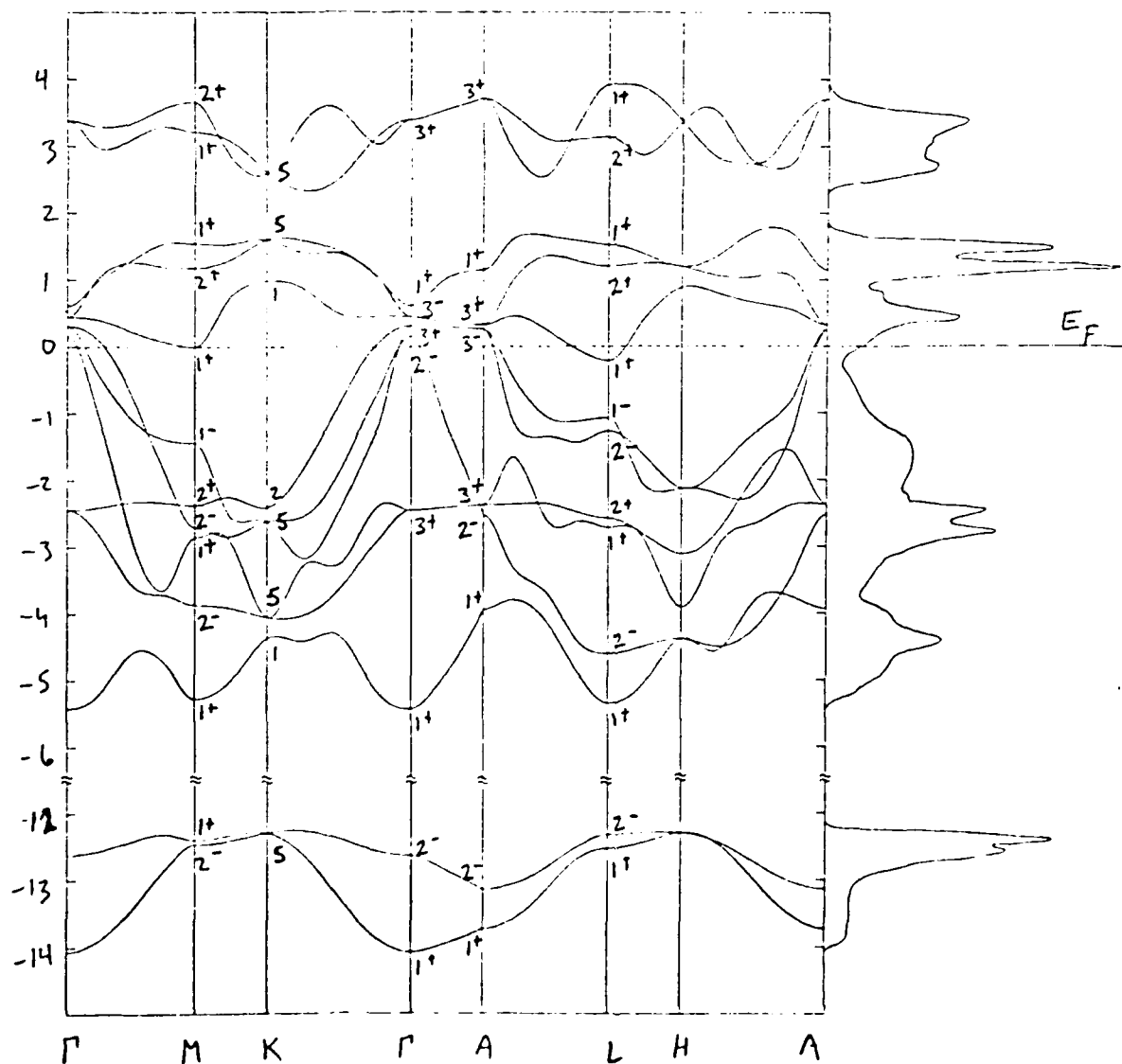


Figure 3

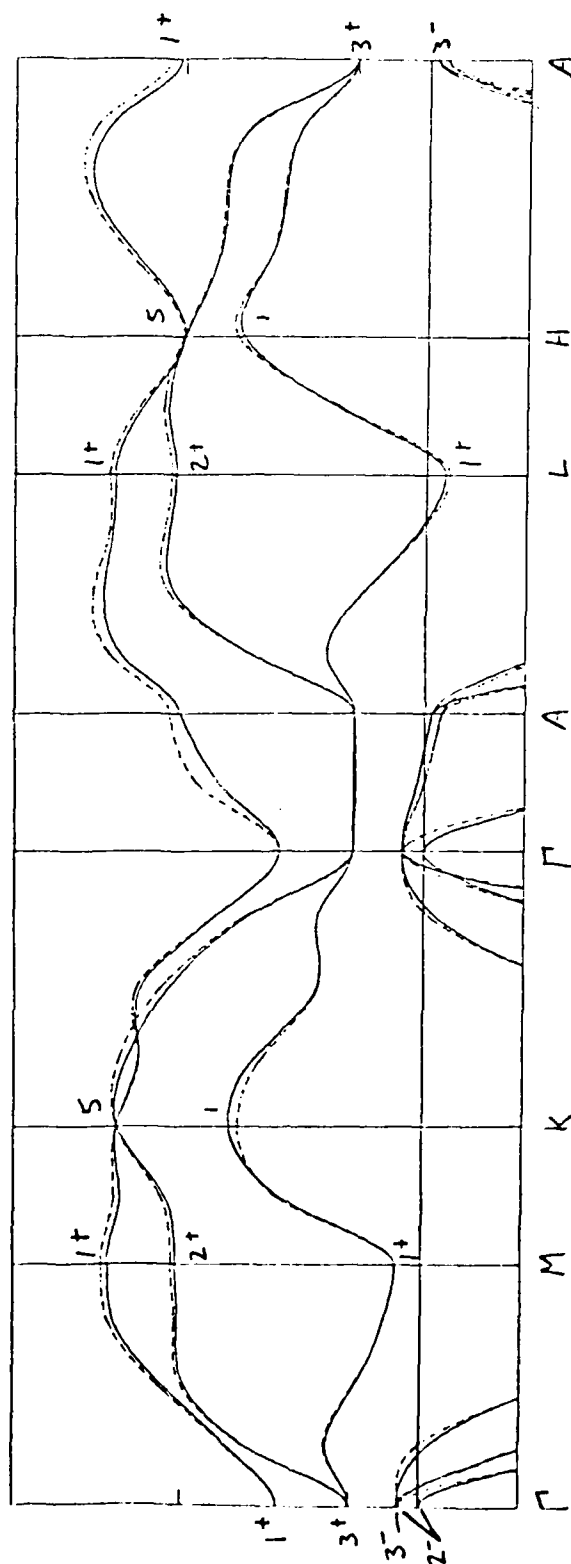
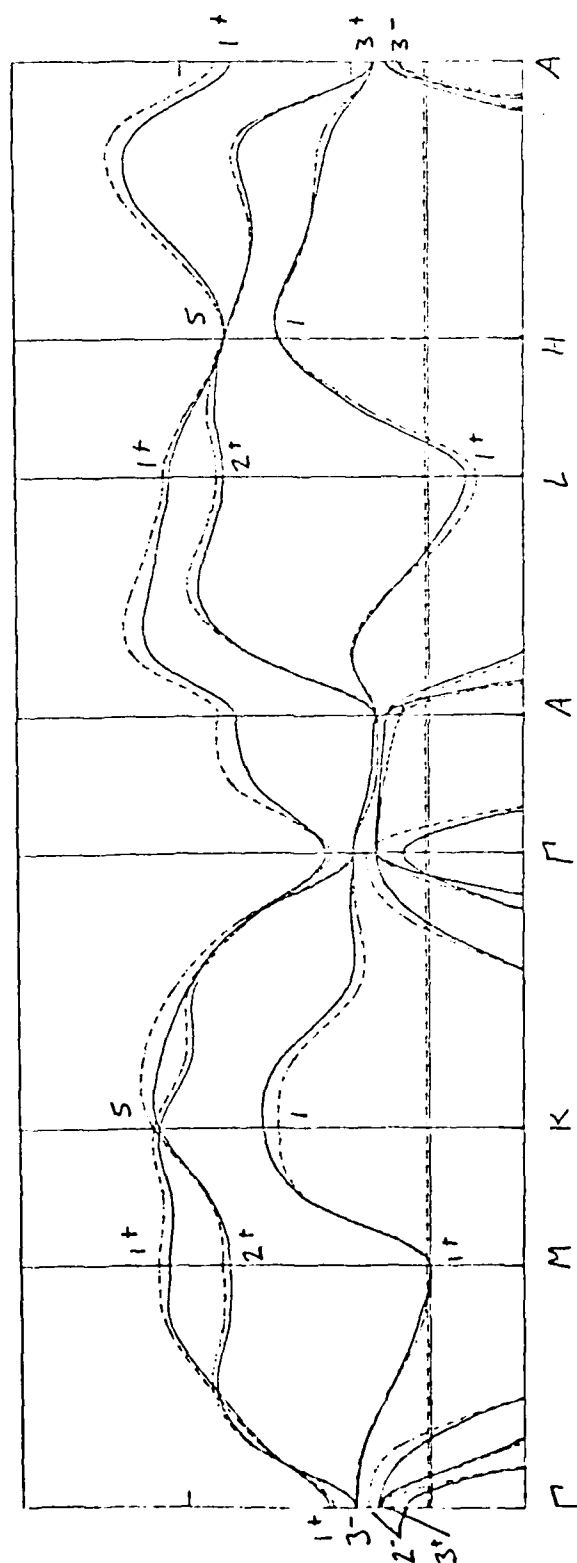




Figure 4



**END**

**FILMED**

**4-85**

**DTIC**